

# Continuum gamma-ray emission from light dark matter positrons and electrons

P. Sizun,<sup>1,\*</sup> M. Cassé,<sup>1,2</sup> and S. Schanne<sup>1</sup>

<sup>1</sup>*DAPNIA/Service d'Astrophysique, CEA Saclay, F-91191 Gif-sur-Yvette Cedex, France*

<sup>2</sup>*Institut d'Astrophysique de Paris, 98 bis Bd Arago, F-75014 Paris, France*

(Dated: November 4, 2019)

The annihilation of light dark matter was recently advocated as a possible explanation of the large positron injection rate at the Galactic center deduced from observations by the SPI spectrometer aboard INTEGRAL. The modelling of internal Bremsstrahlung and in-flight annihilation radiations associated to this process drastically reduced the mass range of this light dark matter particle. We estimate critically the various energy losses and radiations involved in the propagation of the positron before its annihilation—in-flight or at rest.

Using a simple model with mono-energetic positrons injected and confined to the Galactic bulge, we compute energy losses and gamma-ray radiations caused by ionization, Bremsstrahlung interactions as well as in-flight and at rest annihilation and compare these predictions to the available observations, for various injection energies.

Confronting the predictions with observations by the EGRET, COMPTEL, SPI and IBIS/ISGRI instruments, we deduce a new mass upper bound of 25-30 MeV for the hypothetical light dark matter particle. We stress out how the precise limit depends on the degree of ionization of the propagation medium and how crucial morphology studies will be to set more stringent constraints, as simple flux considerations suffer from our poor knowledge of the radiation from unresolved sources and cosmic-ray interactions.

PACS numbers: 95.30.Cq,95.35.+d,95.55.Ka,98.35.-a,98.38.Am,98.70.-f,98.70.Rz,98.70.Sa

## I. INTRODUCTION

Observed by various instruments since the 70's [1], the 511 keV gamma-ray line emission from the Galactic center has now been studied for almost four years with the SPI spectrometer [2] aboard the INTEGRAL satellite. While this emission is definitely the result of electron-positron annihilations in the central region of the Galaxy, the origin of these positrons remains obscure.

What is clear, however, from the spectral analysis of this line, is that most of the positrons are set to rest, form positronium and annihilate in the Galactic bulge (hereafter GB) [3, 4]. Thus, there should be material in the bulge to slow down these leptons, as well as a significant magnetic field to confine them, which is an important information since the interstellar medium in this region is very difficult to observe. As far as positrons are concerned, the main characteristic to explain is their very high injection rate, *i.e.*  $\sim 1.4 \cdot 10^{43} \text{ e}^+ \text{ s}^{-1}$ , as deduced from the 511 keV line flux of  $1.07 \cdot 10^{-3} \text{ ph cm}^{-2} \text{ s}^{-1}$  measured by INTEGRAL/SPI [4]. Though previous instruments like SMM, TGRS, CGRO/OSSE gave essentially the same requirement [1], it is surprising that nobody had remarked that type Ia supernovæ, a long time considered the main source of GB positrons, fall short explaining this high injection rate [5, 6, 7]. Fortunately, this drawback is now taken seriously.

Another clue to the origin of these GB positrons is the

large extent of the emitting region,  $8^\circ$  FWHM [3], indicating that either they emanate from a single central source or a population of sources densely packed in the centre of the Galaxy and diffuse to fill the whole bulge region, or there is a source population with an extension similar or greater than the GB. Indeed, the 511 keV emission region traces where positrons annihilate, and is therefore related to the distribution of the gas in the Galactic bulge.

Potential astrophysical sources of positrons are numerous (SNIa, hypernovæ, gamma-ray bursts, cosmic rays, low mass X-ray binaries, millisecond pulsars, . . .) and we will not discuss them in detail here. None of them qualifies to account for both the flux and morphology of the 511 keV emission. Some candidates are excluded on the basis of the disk over bulge ratio [8] and others like millisecond pulsars [9] and gamma-ray bursts [10] are shaded off, the first because the electrons and positrons would be injected at such energies that their Bremsstrahlung emission would be excessive, and the second because their rate of appearance is insufficient to supply positrons at the required rate, due to the high (solar) metallicity of the GB [11].

In front of this situation, two rather daring hypotheses have been put forward :

- the sources belong to the established list but there is something important not taken into account in the astrophysical scenario. Positrons from the Galactic disk can be transferred to the bulge where they annihilate [8]. However, the transport mechanism from the disk to the centre is poorly known, depending critically on the topology and strength of

---

\*sizun@cea.fr

the large scale magnetic field and on the diffusion coefficient of low energy positrons in the relevant magnetic field [4, 10];

- new sources or mechanisms are required, which are not in the catalog. We will consider this second proposal, and more specifically the light dark matter (hereafter LDM) scenario [5, 6, 12, 13, 14, 15]. Other exotica from the particle physics community include Q balls [16], relic particles [17], decaying axinos [18], primordial black holes [19], color superconducting dark matter [20], superconducting cosmic strings [21], dark energy stars [22], and moduli decays [23]; they will not be discussed here.

Surprisingly, though the 511 keV emission from the GB was first detected more than thirty years ago, it is only with the SPI observations that a great deal of imagination and activity has been triggered among the astroparticle community.

In this contribution, we gather  $\gamma$ -ray observations performed by the CGRO (COMPTEL, EGRET) and INTEGRAL (IBIS/ISGRI, SPI) missions and see what constraints they set on the LDM candidate. A note of warning however: since we are interested in diffuse radiation, the delicate problems of unresolved sources, particularly acute at low energies, and of alternate diffuse sources should always be kept in mind. We do not focus on the morphology of the emission [15, 24], which is a thorny subject, since the dark matter profile is not well established, varying considerably from one author to the other (see e.g. [25, 26], and its distribution could furthermore be clumpy.

We content ourselves to calculate the secondary emission of electrons and positrons in the course of their propagation, the only free parameter being the mass of the LDM particle. Energy losses are central to the problem, since all cross-sections of interest depend on energy, except internal Bremsstrahlung associated to the pair production. We restrict our study to global flux and spectral shape considerations, at the expense of morphology. The main difficulty is not theoretical, but observational: it will be to separate the bulge emission in the continuum from that of the disk, due to cosmic rays.

## II. OVERVIEW

When colliding in the central part of the Galaxy, LDM particles  $\chi$ , with mass  $m_\chi < 200$  MeV, are expected to annihilate into  $e^- - e^+$  pairs. The total energy imparted to the pair is equal to twice this mass  $m_\chi$ , still unknown. Internal Bremsstrahlung in the course of the pair production [27, 28] produces a continuous spectrum independent of the density of the surrounding medium. Due to the mass limitations, both electrons and positrons are intrinsically of modest energy and their energy losses (proportional to the interstellar density) are mainly due to Coulomb interactions with the surrounding medium.

In the course of their propagation, they mainly radiate through the (external) Bremsstrahlung process. Moreover, the released positrons are deemed to annihilate with ambient electrons, producing a definite  $\gamma$ -ray signature (511 keV line plus a low energy continuum). Positron annihilation can occur in flight [29] —in 26% of the cases at most, for  $m_\chi = 200$  MeV— or at rest —mostly through positronium formation. Thus, through the combination of these various mechanisms, a specific  $\gamma$ -ray spectrum, with a discrete and continuous component, is produced by positrons between their creation and their annihilation.

Our aim is to set an upper limit to the mass of the LDM particle self-consistently, by computing this spectrum and confronting it to the observations in the relevant energy range, *i.e.* between  $\sim 10$  keV and 200 MeV. From the particle physics point of view this new constraint, combined with distinct and independent ones coming from big-bang nucleosynthesis [30], type Ia supernovæ, the extra-Galactic hard X-ray and soft  $\gamma$ -ray background [15, 31], should help finding a candidate with the appropriate mass and annihilation cross-section properties.

## III. MODEL

We develop a simple steady-state model adequate for the low energies we are considering, making the reasonable assumption that electrons and positrons below 200 MeV are efficiently confined to the GB, where they annihilate, due to their small gyroradius —a common hypothesis in this field. We also consider that the only positrons present in the GB are produced in situ, at variance with Prantzos [8], who speculates that there could be a transfer of positrons from the disk to the bulge. This daring possibility is very hypothetical since the magnetic field of the Galaxy at large scales and the propagation of low energy positrons are poorly known, as admitted by Prantzos himself. Our problem involves simple physics, repeatedly employed for instance in solar flares physics ([32] and references therein) and Galactic physics [33], and various cross-sections that should be carefully chosen.

### A. Steady-state equilibrium

We consider mono-energetic positrons of total energy  $E_{inj}$  injected in the GB at a rate  $R_{inj}$ . As they travel through the interstellar medium, they lose energy to the ambient medium and can undergo in-flight annihilation. Supposing the positrons are confined in the bulge and neglecting their spatial distribution, the differential number  $N(E)$  of positrons with energy  $E$  in steady-state obeys to the diffusion-loss equation

$$\frac{d}{dE} \left( -N \frac{dE}{dt} \right) = -Q(E), \quad (1)$$

where  $\frac{dE}{dt}$  denotes the mean energy loss rate of positrons and the source term  $Q(E) = R_{inj}\delta(E - E_{inj}) - Q_{IA}(E)$  aggregates the mono-energetic injection and the in-flight annihilation, which is a function of energy:

$$Q_{IA}(E) = n_e \sigma_{IA}(E) v(E) N(E), \quad (2)$$

with  $n_e$  the electron density and  $\sigma_{IA}$  the in-flight annihilation cross-section. Introducing  $g(E) = \frac{n_e \sigma_{IA}(E) v(E)}{-dE/dt}$  and  $G(E) = \int_{E_{inj}}^E g(E') dE' = \log p(E)$ , where  $p(E)$  is the probability for a positron injected at  $E_{inj}$  to survive until energy  $E$ , the number of positrons in the bulge follows from Eq. 1 and 2:

$$N(E) = \frac{R_{inj}}{-dE/dt} e^{G(E)} \quad (mc^2 < E < E_{inj}). \quad (3)$$

We can then obtain the total rate of positrons undergoing in-flight annihilation

$$R_{IA} = \int_{mc^2}^{E_{inj}} Q_{IA}(E) dE = R_{inj} [1 - e^{G(mc^2)}] e^+ s^{-1}, \quad (4)$$

and deduce the rate of annihilation at rest, assuming it equals the rate of positrons reaching complete rest:  $R_A = R_{inj} e^{G(mc^2)} e^+ s^{-1}$ .

## B. Energy losses

The total energy lost by positrons during thermalization goes into various interactions – excitation or ionization, Bremsstrahlung, inverse Compton and synchrotron effects. As their importance varies with the positron's energy, it is mandatory to use refined energy loss rates. For the range of injection energies we are interested in, we can limit ourselves to ionization and Bremsstrahlung.

We stress that the ionization degree  $x_i = n_{HII}/n_H$  in the region of propagation, where  $n_H$  is the hydrogen number density, is of prime importance for the estimate of Coulomb losses [34], since at a given energy they are several times weaker in a neutral medium than in a plasma.

Thus, the total loss rate sums up three terms:

$$\frac{dE}{dt} = \frac{dE^B}{dt}(n_H) + \frac{dE^{I,HI}}{dt}(n_H, x_i) + \frac{dE^{I,HII}}{dt}(n_H, x_i), \quad (5)$$

where the energy lost by a positron due to ionization of neutral matter is taken from [35] while the loss rate for excitation of the ionized component follows [36]. The energy loss caused by Bremsstrahlung interactions is given by Eq. 4BN in [37].

## C. Radiation spectra

### 1. Positron radiation

The total radiation spectrum due to positrons is the sum of five components: the 511 keV line from  $e^+e^-$  an-

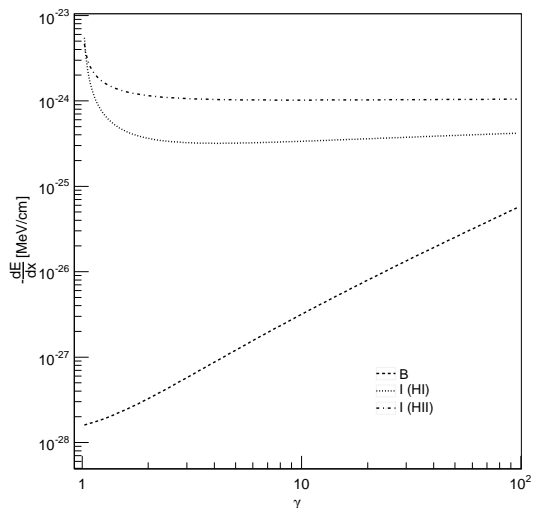


FIG. 1: Energy losses of positrons in a 51% ionized medium ( $n_H = 0.1 \text{ cm}^{-3}$ ). Losses through Coulomb collisions within an ionized medium (I HII) prevail on ionization of the neutral phase (I HI), but both greatly exceed Bremsstrahlung losses (B).

ihilation at rest and from para-positronium decay into  $2\gamma$  (i), the ortho-positronium spectrum from its  $3\gamma$  decay (ii), the continuous spectrum from  $e^+e^-$  in-flight annihilation into  $2\gamma$  (iii), the radiation spectra associated with Bremsstrahlung energy losses (iv) and with the internal Bremsstrahlung taking place in the annihilation process of the dark matter particle (v).

The flux from  $2\gamma$  annihilation at rest  $F^{2\gamma} = 2 \frac{(1-f)+f/4}{4\pi d_{GC}^2} R_A$  is tuned via the injection rate  $R_{inj}$  to the value of  $1.07 \cdot 10^{-3} \text{ ph/cm}^2/\text{s}$  deduced from INTEGRAL observations, where the positronium fraction is constrained to  $f = 93.5\%$  [4].

The  $3\gamma$  ortho-positronium decay spectrum follows

$$\frac{dF^{3\gamma}}{dE_\gamma} = 3 \frac{3f/4}{4\pi d_{GC}^2} R_A \frac{df_{3\gamma}}{dE_\gamma}(E_\gamma), \quad (6)$$

where the spectral distribution  $\frac{df_{3\gamma}}{dE_\gamma}$  was derived by Ore & Powell [38].

Convolving the differential in-flight annihilation cross-section (Fig. 2) with the positron distribution yields the in-flight annihilation component:

$$\frac{dF^{IA}}{dE_\gamma} = \frac{1}{4\pi d_{GC}^2} \int_{E_{min}(E_\gamma)}^{E_{inj}} n_e \frac{d\sigma^{IA}}{dE_\gamma}(E_\gamma, E) v(E) N(E) dE. \quad (7)$$

The external Bremsstrahlung spectrum is derived in a similar way using Koch & Motz [37]'s cross-section 3BN. Dependence on the electron number density  $n_e$  cancels out. Finally, the internal Bremsstrahlung spectrum depends only on the positron injection rate:

$$\frac{dF^{IB}}{dE_\gamma} = \frac{1}{4\pi d_{GC}^2} \frac{1}{\sigma_{tot}} \frac{d\sigma^{IB}}{dE_\gamma}, \quad (8)$$

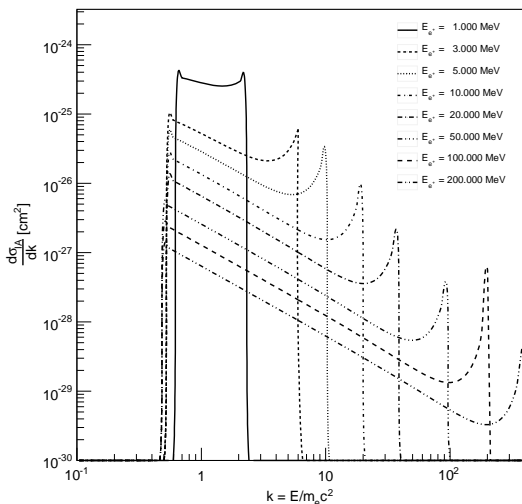


FIG. 2: Differential in-flight annihilation cross-section [39] as a function of the (reduced) photon energy, for various positron energies.

where the required cross-sections have been derived by Beacom et al. [27] and revisited by Boehm & Uwer [28].

## 2. Electron radiation.

In addition to the five positron radiation components comes the Bremsstrahlung spectrum from the mono-energetic electrons injected together with positrons during the dark matter annihilation process, whose equilibrium spectral distribution follows  $N_{e^-}(E) = \frac{R_{inj}}{-dE/dt} (mc^2 < E < E_{inj})$ .

## D. Discussion

Fig. 3 displays the various components of the radiation emitted by positrons and electrons from dark matter annihilation for a specific mono-energetic injection, while Fig. 4 shows the evolution of the total spectrum with increasing injection energies and the influence of the ionization fraction.

As  $\sim 51\%$  of the rest annihilation takes place in the warm ionized phase of the interstellar medium [4], we can assume that the mean degree of ionization of the medium where the thermalizing positrons propagate ranges between 0 and 51%. We consider both extreme cases; the latter one enables us to release constraints on the mass of the dark matter particle.

## IV. CONFRONTATION TO OBSERVATIONS

After computing in § III the total diffuse  $\gamma$ -ray flux caused by the production, interactions and annihilation

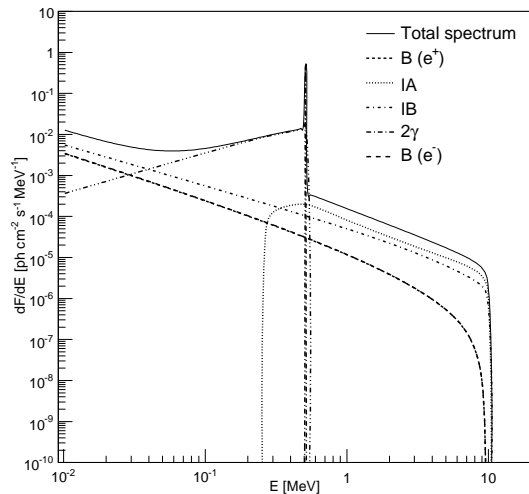


FIG. 3: Light dark matter ( $E_{inj}=10$  MeV) radiation spectra: positron annihilation spectra (in-flight: IA;  $2\gamma$  at rest;  $3\gamma$  at rest), positron energy loss spectra (internal Bremsstrahlung: IB; Bremsstrahlung: B  $e^+$ ), electron Bremsstrahlung spectrum (B  $e^-$ ) and total spectrum (plain).

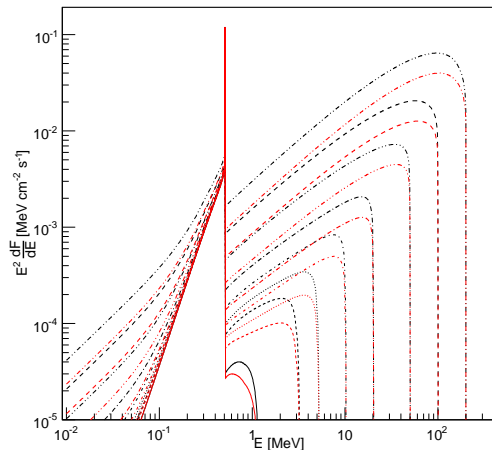


FIG. 4: Total dark matter radiation spectrum for various injection energies  $E_{inj}$  (1, 3, 5, 10, 20, 50, 100 and 200 MeV). In a partially ionized medium (red curves), higher energy losses through ionization lead to lower Bremsstrahlung fluxes.

of positrons and electrons coming from the annihilation of a LDM particle (hereafter the LDM flux), we would like to use observations by INTEGRAL (ISGRI and SPI) and CGRO (COMPTEL and EGRET) to derive some constraints on the mass of this particle. The computed flux stands for the GB, in which we assume that positrons (and associated electrons) are produced and trapped.

Therefore, we would like to show, for each possible injection energy of the positrons (i) whether the available data should and do display an excess in the bulge region with respect to the surrounding Galactic plane and

(ii) whether the total predicted flux exceeds the observed one, taking other gamma-ray diffuse components into account. The latter include extra-Galactic diffuse emission, diffuse emission from the interaction of Galactic cosmic rays (CRs) with the interstellar medium and a component due to —still— unresolved point sources.

As our model does not include spatial diffusion, we adopt a conservative attitude and rely on the available observations, between 20 keV and 200 MeV, of a  $20^\circ \times 20^\circ$  zone centered on the Galactic center, at variance with Beacom & Yüksel [29] who considered a  $5^\circ \times 5^\circ$  zone needing data interpolation. Under the hypothesis that the morphology of the LDM  $\gamma$ -ray emission follows a  $8^\circ$  FWHM Gaussian spatial distribution, as already shown for the 511 keV and positronium components, a  $20^\circ$  wide region includes 99% of the LDM emission and is compatible with the instruments involved. However, in such a region, the LDM flux might be drown in the contributions from CRs and point sources: the contrast between the bulge and the disk is not optimal. By artificially narrowing the beam to a  $5^\circ \times 5^\circ$  solid angle, as in [29], we might enhance the signal to background ratio but with flux statistical uncertainties increasing by a factor of 4.

### A. Total bulge spectrum constraints

Fig. 5 compares the total diffuse  $\gamma$ -ray spectrum expected from the bulge for various masses of the LDM particle —between 1 MeV and 200 MeV— to the diffuse fluxes measured by four instruments. The spectrum predicted by Strong et al. [41, 44] using the cosmic-ray propagation and  $\gamma$ -ray production code GALPROP was integrated over a  $20^\circ \times 20^\circ$  region and added to the LDM model spectrum. The GALPROP model reliably reproduces the measured diffuse spectrum in the EGRET energy range, mostly through the pion decay bump, but fails to account by itself for the detected unresolved flux at lower energies.

We will filter authorized models by requiring that the total LDM and CR flux never *exceeds* the observed flux. It can be noticed however that none of our models has a soft enough spectrum to explain the gap between the GALPROP CR spectrum and the data over the entire 511 keV-200 MeV energy range.

#### 1. INTEGRAL/ISGRI

Analyzing the INTEGRAL/IBIS/ISGRI data, Krivonos et al. [40] computed the Galactic ridge X-ray spectrum in the 17-200 keV range. As the imager, used as a collimated instrument, has a  $19^\circ$  wide 50% coded field of view, the obtained fluxes can be roughly compared to our model. Below 40 keV, after background subtraction and removal of resolved sources, the residual fluxes widely exceed the total model and do not allow

us to derive any constraint : this gap is still matter of debate but is most often attributed to a population of unresolved point sources, like Galactic pulsars. Above 60 keV, no residual flux is detected but three  $2\sigma$  upper limits have been set on the possible unresolved emission. These upper limits, together with the residual flux at 50 keV, permit us to exclude with 95% confidence LDM particle masses over  $\sim 110$  MeV —case of a completely neutral medium— and even  $\sim 70$  MeV —case of a half ionized medium.

#### 2. INTEGRAL/SPI

The INTEGRAL/SPI diffuse spectrum in Fig. 5 was derived by Strong et al. [41] by fitting the instrument's data with a multi-component imaging model including point sources detected by the spectrometer and a set of ten maps with various diffuse morphologies. The discrepancy between the SPI spectrum shown, which sums up the ten diffuse components in our  $20^\circ \times 20^\circ$  region, and the ISGRI fluxes and upper limits could be explained by the imager's better ability to detect faint point sources. When using the GALPROP model as the underlying continuum, the only SPI flux that lets us rule out a specific injection energy is the one derived above the 511 keV annihilation line: from the spectrometer's data, we can exclude with a 95% probability masses over  $\sim 200$  MeV for a neutral medium while those remain acceptable in the frame of an ionized medium.

#### 3. CGRO/COMPTEL

Starting from the COMPTEL  $\gamma$ -ray skymaps in the 1-3, 3-10 and 10-30 MeV energy bands [42], we computed the total diffuse flux in our  $20^\circ$  wide region, subtracting a zero level deduced from high latitudes. The resulting points, whose uncertainties were set to 30% but remain a matter of discussion, give us the most stringent constraints so far, disallowing at a 95% confidence level masses of the LDM particle above 25 MeV —for a neutral medium— or 35 MeV —for a half-ionized medium.

#### 4. CGRO/EGRET

EGRET  $\gamma$ -ray fluxes [43] above 30 MeV —here adapted to our region of study by integration of longitude profiles after subtraction of the isotropic extra-Galactic component— are also a rather limiting factor as cosmic-ray interaction models suffice to explain them: no additional diffuse component such as in-flight annihilation or internal Bremsstrahlung is required, which basically sets the maximum mass of the dark matter particle to the lower energy boundary of EGRET, about 30 MeV.

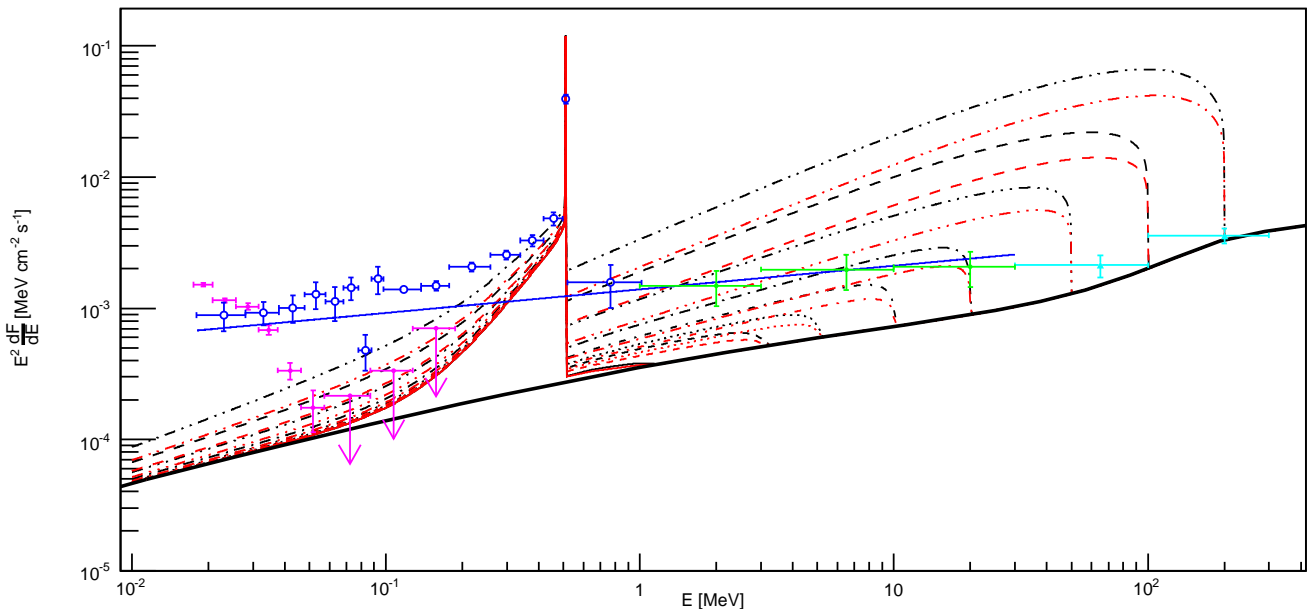


FIG. 5: Comparison between the total diffuse spectrum expected from a  $20^\circ$  wide region at the Galactic center and the diffuse fluxes measured by IBIS (Krivonos et al. 2006 [40]; magenta), SPI (Strong et al. 2005 [41]; blue), COMPTEL (Strong et al. 1999 [42]; green) and EGRET (Hunter et al. 1997 [43]; cyan). The model curves (thin lines) are the sum of the CR interactions component computed by Strong [41] (black thick line), and the dark matter related component, computed in § III for injection energies  $E_{inj} = 1, 3, 5, 10, 20, 50, 100$  and  $200$  MeV, in a neutral (black) or 51% ionized medium (red).

## B. Morphological constraints

The approach we adopted leads to a maximum injection energy of positrons at the Galactic center of  $\sim 30$ – $40$  MeV which is not very constraining and leaves open a mass window for the hypothetical LDM particle. However, it is only based on global flux considerations and has the drawback of leaving completely out of consideration the disturbing fact that, outside the energy range of the positronium [45] and the 511 keV line [3], no continuum excess has been detected in the bulge with respect to the surrounding Galactic plane while the hypotheses of our model require positrons to be confined to the bulge, as is the case for their  $\gamma$ -ray emission.

Therefore, taking note of the more disc-like than bulge-like morphology suggested by COMPTEL skymaps and profiles above 1 MeV, we could conclude that most of the emission detected by both COMPTEL and SPI have their origin in either unresolved faint point sources or diffuse mechanisms other than those related to LDM particles. Assuming a relative uniformity of this  $\gamma$ -ray background along the Galactic plane, we can find the powerlaw best fitting the SPI and COMPTEL data and use it as a base for our model to see whether the potential additive emission caused by LDM particles in the bulge remains within data uncertainties.

This second approach, used by Beacom & Yüksel [29], is shown in Fig. 6 but still for a  $20^\circ$  wide region. Instead of adding the GALPROP cosmic-ray induced spectrum to

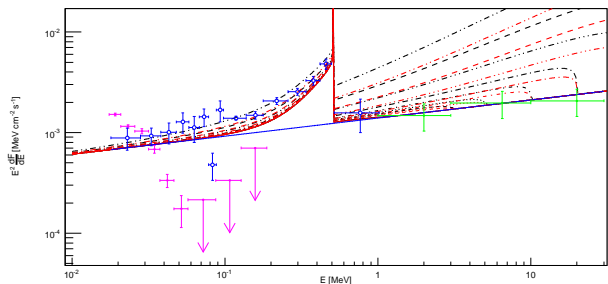


FIG. 6: Comparison between the total diffuse spectrum expected from a  $20^\circ$  wide region at the Galactic center and the diffuse fluxes measured by IBIS (magenta), SPI (blue) and COMPTEL (green). Instead of taking the predictions from cosmic-ray interaction codes as a base level for our LDM model like in Fig. 5, we now use a powerlaw-like (blue line)  $\gamma$ -ray background —already displayed in Fig. 5— compatible with SPI and COMPTEL data, as in [29].

our model as in § IV A, we added the powerlaw derived by Strong et al. [41] for the complete SPI unresolved spectrum. We can thus derive more stringent constraints: COMPTEL points lead to a maximum injection energy of  $\sim 10$  MeV (95% CL). However, even if such a powerlaw is compatible with both the SPI and COMPTEL instruments, its relevance is hindered by its incompatibility with the upper limits set by ISGRI on the unresolved emission at lower energies.

Going a step further is possible, by making assumptions on the distribution of the LDM flux within the bulge. Beacom & Yüksel, assuming the same Gaussian morphology found for the  $2\gamma$  and the ortho-positronium is valid for the rest of the LDM flux, scaled their model and allowed themselves to consider a smaller region, with a smaller portion of diffuse background, and thus to derive more stringent constraints. We will not go this far but simply underline how the handling of uncertainties becomes crucial in such a framework. Indeed, because the  $\sim 36\%$  error on the SPI high energy flux is *mostly statistical*, when extrapolating the flux to a smaller region, its relative error will grow like the square root of the inverse ratio between the solid angles of the two regions, *e.g.* by a factor 4 for a  $5^\circ \times 5^\circ$  zone.

A thorough study of the morphological aspects of in-flight annihilation would in fact require a more complete model, taking spatial diffusion as well as energy losses into account. This would allow us to take full advantage of the morphological information contained in the data.

## V. CONCLUSIONS

Combining all the radiation components related to LDM particles —mostly in-flight annihilation and internal Bremsstrahlung— we were able to set a conservative upper bound of 25-30 MeV on the mass of these particles, based on EGRET and COMPTEL data.

A previous study by Beacom & Yüksel [29] had concluded on a 3 MeV upper mass, thus completely ruling out the LDM hypothesis considering that cooling dynamics of core collapse supernovæ disfavour masses below  $\sim 10$  MeV [13]. The main reasons for our different conclusion come from hypotheses on the origin, flux and morphology of the diffuse or unresolved emission *underlying* the LDM radiation and from the handling of flux uncertainties.

We also stressed out the influence of the ionization degree of the interstellar medium on the amplitude of the in-flight radiation spectrum : taking into account the ionization fraction of the propagation region allows

slightly larger values of the mass of the LDM particle.

Moreover, the present conclusions were derived under the demanding assumption that light dark matter annihilation alone accounts for all of the 511 keV line in the Galactic center region. A multi-source scenario would enable us to reduce the amplitude of the LDM  $\gamma$ -ray continuum and to release once again the limit on the LDM particle mass.

*Prospects* In order to further restrict the LDM particle mass range with the INTEGRAL satellite, a refined appraisal of the contribution of faint point sources in the 50-511 keV energy range is required. In this perspective, the census to come of sources found by the imager above 100 keV [46] will be paramount to fine-tune ISGRI upper limits on diffuse emission. Because the spectrometer does not have the capacity to resolve as many faint sources, an increased recognition of ISGRI detections in the analysis of SPI data might prove necessary.

Beyond flux considerations, whose precision is hindered by our uncertain knowledge of the radiation from cosmic-ray interactions and unresolved sources, morphology studies will be a key point to find out whether the 511 keV to 8 MeV energy range presents a faint excess in the GB.

In order to take all aspects of LDM into account, the present model could be extended to include spatial diffusion of positrons and electrons during thermalization and model the differences in the morphologies of the LDM emission at various energies. Furthermore, studying the influence of the in-flight annihilation and internal Bremsstrahlung components on the positronium fraction derived [4] from SPI data would be interesting.

## Acknowledgments

The authors thank A. W. Strong for making available COMPTEL and SPI results as well as the GALPROP model. We are also grateful to P. Fayet, F. A. Aharonian, B. Cordier, F. Lebrun, J. Paul and P. Jean for discussions on in-flight annihilation, energy losses and observational data uncertainties.

- 
- [1] P. A. Milne (2006), astro-ph/0603006.
  - [2] G. Vedrenne et al., A&A **411**, L63 (2003).
  - [3] J. Knödlseeder et al., A&A **441**, 513 (2005).
  - [4] P. Jean et al., A&A **445**, 579 (2006).
  - [5] M. Cassé et al., ApJ **602**, L17 (2004), astro-ph/0309824.
  - [6] S. Schanne et al., Adv. Space Res. pp. 2307–+ (2005), astro-ph/0411454.
  - [7] S. Schanne et al., in *ESA SP-552* (2004), pp. 73–+.
  - [8] N. Prantzos, A&A **449**, 869 (2006), astro-ph/0511190.
  - [9] W. Wang, Z. J. Jiang, and K. S. Cheng, MNRAS **358**, 263 (2005).
  - [10] E. Parizot et al., A&A **432**, 889 (2005).
  - [11] S. E. Woosley and A. Heger, ApJ **637**, 914 (2006).
  - [12] C. Boehm, D. Hooper, J. Silk, M. Casse, and J. Paul, Phys. Rev. Lett. **92**, 101301 (2004).
  - [13] P. Fayet, D. Hooper, and G. Sigl, Phys. Rev. Lett. **96**, 211302 (2006).
  - [14] M. Cassé and P. Fayet, in *EAS Pub. Series* (2006), pp. 201–208.
  - [15] Y. Rasera, R. Teyssier, et al., Phys. Rev. D **73**, 103518 (2006).
  - [16] S. Kasuya and F. Takahashi, Phys. Rev. D **72**, 085015 (2005).
  - [17] C. Picciotto and M. Pospelov, Physics Letters B **605**, 15 (2005).
  - [18] D. Hooper and L.-T. Wang, Phys. Rev. D **70**, 063506

- (2004).
- [19] P. H. Frampton and T. W. Kephart, *Mod. Phys. Lett. A* **20**, 1573 (2005), hep-ph/0503267.
- [20] D. H. Oaknin and A. R. Zhitnitsky, *Phys. Rev. Lett.* **94**, 101301 (2005).
- [21] F. Ferrer and T. Vachaspati, *Phys. Rev. Lett.* **95**, 261302 (2005), astro-ph/0505063.
- [22] G. Chapline (2005), astro-ph/0503200.
- [23] M. Kawasaki and T. Yanagida, *Physics Letters B* **624**, 162 (2005), hep-ph/0505167.
- [24] C. Boehm and Y. Ascasibar, *Phys. Rev. D* **70**, 115013 (2004).
- [25] J. F. Navarro, C. S. Frenk, and S. D. M. White, *ApJ* **490**, 493 (1997), astro-ph/9611107.
- [26] B. Moore et al., *MNRAS* **310**, 1147 (1999), astro-ph/9903164.
- [27] J. F. Beacom, N. F. Bell, and G. Bertone, *Phys. Rev. Lett.* **94**, 171301 (2005).
- [28] C. Boehm and P. Uwer (2006), hep-ph/0606058.
- [29] J. F. Beacom and H. Yüksel (2005), astro-ph/0512411.
- [30] P. D. Serpico and G. G. Raffelt, *Phys. Rev. D* **70**, 043526 (2004), astro-ph/0403417.
- [31] K. Ahn and E. Komatsu, *Phys. Rev. D* **71**, 021303(R) (2005).
- [32] R. J. Murphy et al., *ApJ* **161**, 495 (2005).
- [33] J. G. Skibo et al., *A&AS* **120**, C403+ (1996).
- [34] A. Soutoul and P. Ferrando, in *AIP Conf. Proc. 183* (1989), pp. 400–+.
- [35] Longair, M. S., *High Energy Astrophysics* (Cambridge, 1992), 2nd ed.
- [36] F. A. Aharonian and A. M. Atoyan, *Soviet Astr. Lett.* **7**, 395 (1981).
- [37] H. W. Koch and J. W. Motz, *Rev. of Modern Phys.* **31**, 920 (1959).
- [38] A. Ore and J. L. Powell, *Phys. Rev.* **75**, 1696 (1949).
- [39] F. A. Aharonian and A. M. Atoyan, *Phys. Lett. B* **99**, 301 (1981).
- [40] R. Krivonos et al. (2006), astro-ph/0605420.
- [41] A. W. Strong et al., *A&A* **444**, 495 (2005).
- [42] A. W. Strong et al., *ApLC* **39**, 209 (1999).
- [43] S. D. Hunter et al., *ApJ* **481**, 205 (1997).
- [44] A. W. Strong et al., *ApJ* **613**, 962 (2004).
- [45] G. Weidenspointner et al., *A&A* **450**, 1013 (2006).
- [46] A. Bazzano et al. (2006), in prep.